

# Journal of Biomedical Optics

[SPIEDigitalLibrary.org/jbo](http://SPIEDigitalLibrary.org/jbo)

## **Terahertz sensing in corneal tissues**

David B. Bennett  
Zachary D. Taylor  
Pria Tewari  
Rahul S. Singh  
Martin O. Culjat  
Warren S. Grundfest  
Daniel J. Sassoon  
R. Duncan Johnson  
Jean-Pierre Hubschman  
Elliott R. Brown

# Terahertz sensing in corneal tissues

David B. Bennett,<sup>a</sup> Zachary D. Taylor,<sup>a</sup> Pria Tewari,<sup>a</sup> Rahul S. Singh,<sup>a</sup> Martin O. Culjat,<sup>a</sup> Warren S. Grundfest,<sup>a</sup> Daniel J. Sassoon,<sup>b</sup> R. Duncan Johnson,<sup>b</sup> Jean-Pierre Hubschman,<sup>b</sup> and Elliott R. Brown<sup>c</sup>

<sup>a</sup>University of California, Los Angeles, Center for Advanced Surgical and Interventional Technology, Los Angeles, California 90095

<sup>b</sup>University of California, Los Angeles, Jules Stein Eye Institute, Los Angeles, California 90095

<sup>c</sup>Wright State University, Department of Physics and Electrical Engineering, Fairborn, Ohio 45435

**Abstract.** This work introduces the potential application of terahertz (THz) sensing to the field of ophthalmology, where it is uniquely suited due to its nonionizing photon energy and high sensitivity to water content. Reflective THz imaging and spectrometry data are reported on *ex-vivo* porcine corneas prepared with uniform water concentrations using polyethylene glycol (PEG) solutions. At 79% water concentration by mass, the measured reflectivity of the cornea was 20.4%, 14.7%, 11.7%, 9.6%, and 7.4% at 0.2, 0.4, 0.6, 0.8, and 1 THz, respectively. Comparison of nine corneas hydrated from 79.1% to 91.5% concentration by mass demonstrated an approximately linear relationship between THz reflectivity and water concentration, with a monotonically decreasing slope as the frequency increases. The THz-corneal tissue interaction is simulated with a Bruggeman model with excellent agreement. THz applications to corneal dystrophy, graft rejection, and refractive surgery are examined from the context of these measurements. © 2011 Society of Photo-Optical Instrumentation Engineers (SPIE). [DOI: 10.1117/1.3575168]

Keywords: terahertz imaging; terahertz reflectometry; corneal health; hydration sensing.

Paper 11006R received Jan. 5, 2011; revised manuscript received Mar. 17, 2011; accepted for publication Mar. 18, 2011; published online May 10, 2011.

## 1 Introduction

Research in the generation, detection, and useful applications of terahertz (THz) (0.1 to 10 THz band) radiation is a relatively new and expanding field of study, with growing attention to the unique sensitivity of THz radiation to water. Reflection-mode THz imaging has come into particular interest because of the high degree of water content sensitivity that can be achieved, as well as the difficulty of transmission-mode medical sensing due to the prohibitively strong attenuation in most biological tissues. Hydration-related variations in dielectric function have been measured in different tissue types and between diseased and healthy tissues, and many of these have been successfully realized using reflection-mode THz sensing.<sup>1</sup> These include imaging and/or spectroscopy of carcinoma, melanoma, skin burns, inflammation, and scarring.<sup>2-6</sup>

The cornea is the eye's outermost structure and is the location of several debilitating disease processes, many of which can permanently damage or impair vision. It has a thickness of roughly 0.55 mm, and provides 46 of the average 59 total diopters of its refractive power.<sup>7,8</sup> The clarity of this tissue is vitally important to its function and is strongly dependent on its relative hydration. The water content of the cornea is regulated by both passive and active mechanisms to preserve its essential transmission and focusing properties. The abnormal elevation of the water concentration of the cornea by an injury or disease process results in corneal edema, which renders the normally clear cornea cloudy, thus blurring vision. It can also lead to swelling of the outer epithelial layer, which often results in severe pain and renders the normally smooth surface rough.

The flow of water through the cornea is also a strong factor in supplying the cells of the cornea with nutrients, transporting leukocytes and other cells responsible for immune response and wound healing, and regulating tear tonicity and osmotic flow from the aqueous humor.<sup>9,10</sup> An understanding of the hydrodynamics of the cornea is fundamental to research in vision, ocular biology, contact-lens design, and pharmaceutical disciplines.

With its ability to noninvasively make direct measurements of the water content of the cornea, THz hydration monitoring has great potential to provide the tools to assess the onset and evolution of disease and the impact of clinical processes and treatments which affect the hydration of the eye. These tools may assist in the diagnosis and treatment of dystrophies, degenerations, injuries, and corneal graft rejection. All of these diseases produce marked changes in the water content of the cornea, as well as location-varying responses that progress with the severity of the disease. If sufficient sensitivity can be achieved, THz sensing may also allow early detection and intervention, which in some cases can prevent irreversible damage and permanent loss of sight. THz sensing may also be helpful for evaluating contact lenses, eye drops, and other products, which are designed to preserve the healthy hydration balance in the cornea.

Current clinical practice estimates corneal hydration by extrapolation from central corneal thickness (CCT) measurements. CCT correlates with water content because the corneal tissue must swell/contract to accommodate the amount of fluid present. This swelling can be measured using ultrasound or optical pachymetry. The extrapolation function which empirically links CCT to corneal hydration is a linear fit between CCT and the average water content of the eye which was established in the 1960s by measuring both in 11 human corneas from an eye

Address all correspondence to: David B. Bennett, University of California Los Angeles, Electrical Engineering, 10833 Le Conte Avenue, Suite BH-826, Los Angeles, California 90095-1594. Tel: 805 386 3896; Fax: 310 206 8823; E-mail: dbennett.mednit@gmail.com.

bank.<sup>11</sup> This function is given as:

$$h = \frac{m_{\text{H}_2\text{O}}}{m_{\text{dry cornea}}} = 7.0(\text{CCT}_{\text{mm}}) - 0.64, \quad (1)$$

where  $h$  is the water-to-dry tissue ratio,  $m_{\text{H}_2\text{O}}$  and  $m_{\text{dry cornea}}$  are the masses of water and dry corneal tissue in the cornea, and  $\text{CCT}_{\text{mm}}$  is the central corneal thickness in millimeters.<sup>12</sup> This equation can be rearranged to give the absolute water concentration  $H$ :

$$H = \frac{m_{\text{H}_2\text{O}}}{m_{\text{H}_2\text{O}} + m_{\text{dry cornea}}} = \frac{(\text{CCT}_{\text{mm}}) - 0.091}{(\text{CCT}_{\text{mm}}) + 0.051}. \quad (2)$$

Since the  $\text{CCT}_{\text{mm}}$  in human corneal tissues is about 0.56 mm, Eq. (2) shows a weak dependence of  $H$  on  $\text{CCT}_{\text{mm}}$ . The best-case hydration sensitivity of optical and ultrasound pachymetry can be estimated using a study in which multiple physicians measured the CCT of patients by both methods and assessed the repeatability. Accuracy values of 11.9 and 9.9  $\mu\text{m}$  for optical and ultrasound pachymetry, respectively, were found, and therefore Eq. (2) estimates hydration sensitivities of 0.5% and 0.4%, respectively.<sup>13</sup>

By contrast, hydration monitoring employing THz reflectivity would utilize the interaction between the probe beam and water itself instead of a secondary manifestation of the presence of water as in CCT measurements. As such, THz is expected to be more robust against physiological variations in corneal thickness between patients, including differences because of age, disease states, and environmental factors. It is also not subject to the uncertainty inherent to the pachymetry modalities (optical or ultrasonic) that are themselves modified by changes in hydration through variations in the refractive index and the speed of sound, respectively.<sup>14</sup>

The purpose of this paper is to demonstrate that THz sensing can be used to assess corneal hydration, and to quantify the relationship between corneal hydration and THz reflectivity. This will allow the sensitivity of THz hydration sensing in the cornea to be determined and the penetration depth of the radiation to be predicted. This sensitivity will be compared to the sensitivity of the current clinical approaches of ultrasound and optical pachymetry. The penetration depth and sensitivity will also be discussed in the context of current hydration-sensing needs in clinical ophthalmology, including diagnosis of corneal dystrophies and graft rejection events. Further clinical applications may be found in laser refractive surgery techniques such as LASIK, in which the ablation rate of the surgical laser exhibits a dependency on corneal tissue hydration.<sup>15</sup> If remote sensing of corneal hydration by THz reflectometry can be developed, it may lead to tools to provide the surgical laser system with feedback to better control the ablation of tissue. This marks the first time that THz hydration monitoring has been quantitatively evaluated for applications in clinical ophthalmology.

## 2 Methods

THz imagery and spectra were obtained in this study using two THz systems. The imagery was used to demonstrate the detection of tissue hydration by THz reflectometry with all other factors held constant, and the spectroscopy data was obtained to

quantify the sensitivity of THz reflectometry to water concentration across the THz spectrum.

### 2.1 THz Imaging System

THz imagery was acquired using a compact imaging system that employs a photoconductive switch pumped by a 780 nm mode-locked fiber laser [pulse width = 230 fs, pulse repetition frequency (PRF) = 20 MHz, average power = 7.5 mW] described in detail elsewhere.<sup>16</sup> The emitted THz radiation is directed to the sample at an angle of 14 deg from vertical through a chain of off-axis parabolic mirrors and then detected by a zero-bias Shottky rectifier (Virginia Diodes, Charlottesville, Virginia). The net power spectrum of this configuration has a center frequency of 525 GHz and an effective bandwidth of 125 GHz, which is sufficient to overcome interference from standing waves while still providing good spatial resolution ( $\sim 1.2$  mm, 10% to 90% spot size).<sup>17</sup> The choice of center frequency of our system is motivated by the tradeoff between water concentration sensitivity, robustness to scattering, and spatial resolution, which are observed to be well balanced at 525 GHz.<sup>18</sup> THz imagery of a  $35 \times 35$  mm area can be obtained in 110 s.<sup>19</sup>

### 2.2 THz Spectroscopy System

THz spectroscopy data was obtained using a commercial time domain spectroscopy system (TPS Spectra 3000 CF system, TeraView). This system uses a proprietary photoconductive transceiver pumped by a Ti:Sapphire mode-locked laser (pulse width = 90 fs, PRF = 80 MHz, average power = 280 mW). It has a reflection-mode module that is used to acquire reflection data from a sample with an incidence and reflection angle of 30 deg from the vertical. The reflected waveform from a target is obtained by optoelectronic sampling, which can acquire a spectrum in 1 s with a frequency resolution of 6 GHz.

### 2.3 THz Imaging of Evaporative Drying in an Ex Vivo Porcine Cornea

The THz imaging system was first used to monitor the loss of water by evaporation in an *ex-vivo* porcine cornea. To isolate the water contrast from all other factors, the drying mount illustrated in Fig. 1 was constructed which pressed a hydrated cornea against a fixed, transparent quartz imaging window (Meller Optics, Providence, Rhode Island) and allowed images to be taken in this constrained geometry over the course of several hours. This apparatus removes the effects of many sources of variation unrelated to hydration change, including topology, curvature, and the standoff distance between sample and imaging head. A porcine cornea was dissected from an eye and soaked in deionized water for 1 h followed by drying and re-soaking. The cornea was then allowed to dry on a mass balance (ZSA 80, Scientech, Boulder, Colorado) at room temperature. At preset increments, the cornea was removed from the scale, mounted on the window, and imaged. The window was cleaned with acetone and methanol between each scan. The average (inhomogeneously distributed) water concentration was determined by mass measurement on the scale (accuracy  $\pm 1$  mg, giving an error of  $<0.53\%$  water concentration for the entire cornea set which had hydrated masses of 190 mg and above).

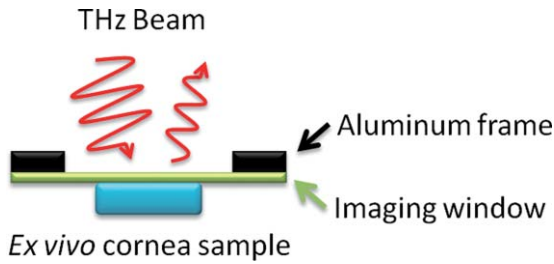


**Fig. 1** Illustration of experimental geometry for THz imaging and spectroscopy of *ex vivo* corneal tissues.

#### 2.4 THz Sensitivity to Hydration in Corneal Tissues

In order to measure the nominal sensitivity of reflection-mode sensing in the THz band to water concentration in the cornea, reflection-mode spectroscopy of *ex-vivo* porcine corneas dissected by the same method as in Sec. 2.3 was performed on nine samples at different hydration levels. This experiment requires the water concentrations of the cornea samples to be homogeneous so they can be computed using a mass measurement without the kind of spatial variation seen in the previous experiment (see Fig. 2). Following the work of Meek et al.,<sup>20</sup> nine corneas were soaked in a 0%, 3%, 5%, and 7% polyethylene glycol (PEG) solutions containing 0.15M NaCl for 3 days. The concentrations of these solutions produce different equilibrium water concentrations in the corneas that varied between 79.1% and 91.5%. The corneas were mounted on a window frame in a similar manner as illustrated in Fig. 1, with the quartz window replaced by a tightly-stretched 12.7- $\mu\text{m}$  mylar film. Abutting

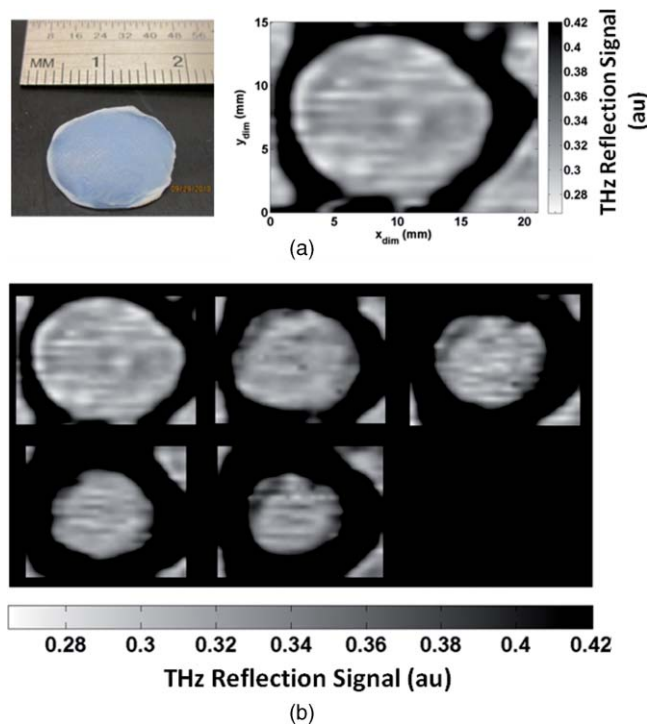


**Fig. 2** (a) Optical and THz image of a hydrated *ex vivo* cornea. (b) THz image of an *ex vivo* porcine cornea at (upper-left to lower-right) 84.74%, 78.64%, 75.27%, 70.25%, and 66.06% water content by mass.

the cornea against this thin film forced it into a flat, orthogonal geometry with respect to the THz optics. The mylar window produces little perturbation to the passing beam because the window is optically thin with respect to the wavelengths of inquiry (mylar index  $\approx 1.67$ , thickness  $< \lambda/10$  up to 1.4 THz).<sup>21</sup> THz spectroscopy data was obtained using the TeraView time-domain system. The relation between water concentration and THz reflectivity was computed from this data, and the absolute sensitivity of our system was predicted.

#### 2.5 Simulation of THz-Corneal Tissue Interaction and the Penetration Depth in Corneal Tissues

The reflectivity spectrum of a hydrated corneal tissue can be simulated using a Bruggeman effective media model which combines the basic constituents of the cornea. The details of Bruggeman analysis and its application to biological tissue are discussed elsewhere.<sup>22</sup> A useful model of the cornea system is a binary mixture of water and biological background material. The dielectric function of both of these materials is known from the literature. The double-Debye model of water describes the dielectric response of the water in the cornea,<sup>23</sup> and the refractive index of corneal tissue with the water removed was measured as approximately 1.55.<sup>24</sup> Following the analysis in Bennett et al.,<sup>22</sup> the reflection from a homogeneous mixture of corneal tissue and water behind a 12.7- $\mu\text{m}$  mylar window is computed for the cornea which is hydrated to a water concentration of 79.1% by mass, which approximately matches the physiological norm *in vivo*.<sup>25</sup> This model will assume that the PEG solution preparation successfully prepares the corneal tissue to a homogeneous water concentration, and so the tissue can be approximated as having a uniform water concentration. This assumption will be verified by imaging one of the corneas.

This model is compared to the measured spectrum, and then used to compute the penetration depth of THz radiation in cornea tissue. For a wave traveling through a medium of complex dielectric function  $\epsilon_r$  in the  $z$ -direction, the electric field and intensity can be written in the form:

$$E = E_0(x, y)e^{-j(\omega/c)\sqrt{\epsilon_r}z}$$

$$I = I_0(x, y)e^{-(2\omega/c)|\text{Im}(\sqrt{\epsilon_r})|z}$$
(3)

where  $\omega$  is the angular frequency,  $c$  is the speed of light, and the imaginary part of  $\sqrt{\epsilon_r}$  is written in this absolute value form [since  $\text{Im}(\sqrt{\epsilon_r}) \leq 0$  here] to emphasize the exponential attenuation behavior. The attenuation behavior of a medium for a given radiation frequency  $\omega$  can be described in terms of the medium's half-value-layer ( $\delta_{\text{HVL}}$ ). The half-value layer is a penetration metric common to clinical radiology which gives distance in a medium which attenuates the power of incident radiation by half,<sup>26</sup> and can be computed by:

$$\delta_{\text{HVL}} = \frac{c \ln(2)}{2\omega|\text{Im}(\sqrt{\epsilon_r})|}$$
(4)

These figures are discussed below in terms of the severity and affected tissue regions of several corneal disease processes to assess the usefulness of THz imaging for diagnosis and monitoring of corneal disease.

### 3 Results

#### 3.1 THz Imaging of Evaporative Drying in a Porcine Cornea

The results of the corneal drying experiment are shown in Fig. 2, with the cornea represented by the entire oval-shaped area centered in the window. The corneal tissue is fully hydrated in the initial scan, and therefore appears bright across the entire image. Clear preferential drying from the outer edges is then seen in the images that follow, as the dark “dry” border closes further inwards toward the center with each subsequent frame. The colorbar scale is inverted with respect to the other images in this study because the refractive index of a hydrated cornea is much larger than that of a dehydrated cornea, and when both are viewed through quartz ( $n = 2.11$ ),<sup>27</sup> the larger mismatch exists between the quartz and the dehydrated cornea. The reflection through quartz is therefore stronger for a dry cornea (smaller index) than a hydrated one (larger index) because the reflection strength depends on the magnitude of the difference. When both corneas are viewed through air ( $n = 1$ ), the larger air/hydrated-cornea mismatch provides the larger reflection. The remainder of the images will be acquired through an optically small mylar window in free space, for which hydrated tissue reflects the most strongly.

The lateral edges of the cornea sample suffer evaporative loss from exposure to air in addition to losses from the epithelial and endothelial surfaces. The progression of drying from the outside-inward is the expected result of the faster diffusion in the lateral directions relative to the thickness direction.<sup>10,28</sup> This is also in accordance with observations from a previous preliminary study in which a single cornea was imaged at a one point in time without constraining its geometry.<sup>29</sup>

#### 3.2 THz Sensitivity to Corneal Hydration

The corneas prepared in the PEG solutions reached water concentrations of 78.8%, 79.1%, 81.0%, 82.4%, 86.9%, 88.7%, 89.0%, 90.0%, and 91.5%. A THz image of one of these corneas is shown in Fig. 3, with the cornea on the right and a piece of microscope cover glass on the left as a reference. Fresnel’s equations predict a 13% reflectivity at a 30 deg incidence angle for glass and this is a near match for the predicted THz reflectivity of a 78% hydrated cornea using the Bruggeman model.<sup>27,30,31</sup>

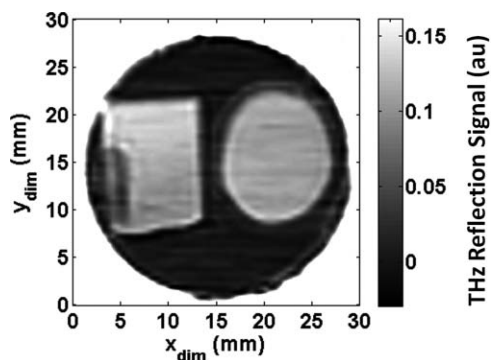


**Fig. 3** Image of porcine cornea (right) prepared by soaking in a PEG solution and a glass square for calibration (left) affixed with glue (tall dark spot on left edge).

In this image, the entire cornea shows a uniform intensity, indicating that the THz reflectivity and the water concentration that it reflects is uniform across the entire cornea. This demonstrates the effectiveness of the PEG technique in yielding samples of high spatial uniformity with respect to hydration.

The spectroscopy results from scanning the cornea samples using the TeraView system are shown in Fig. 4. A clear decrease in reflected intensity is seen in the corneas with reduced amounts of absorbed water at all frequencies. This THz spectrum was observed to be constant as the beam was moved around on the surface of the cornea, again indicating that the equilibration process was successful in uniformly distributing the water throughout the cornea.

From this data, it is possible to calculate the intrinsic sensitivity of THz imaging systems to corneal hydration. Each frequency value along the  $x$ -axis intercepts the reflectivity curves from nine different corneas. These nine points can be plotted to describe the relation between THz reflectivity and corneal hydration at that frequency. This relationship is shown at five frequencies in Fig. 5. The relationships are approximately linear, and the slope of each linear trendline gives the THz reflectivity change characteristic of a unit change in the water concentration at that frequency. Both the reflectivity magnitude and the slope of these linear fits decrease with increasing frequency. This is an example of one of the key trade-offs in THz imaging of hydrated materials. Higher frequencies are capable of producing images with finer spatial resolution, but lower frequencies are more strongly reflected by water and therefore produce both higher reflected signal and more contrast to small water concentration changes.

The slope of the reflectivity-concentration relationship is plotted against frequency in Fig. 6. This curve describes the decreasing sensitivity of THz sensing to water content as frequency increases. For example, a THz reflection measurement at 200 GHz must be able to resolve a minimum of a 0.32% reflection change in order to detect a water concentration change of 1% in a sample. The same water concentration sensitivity would require 0.17% reflectivity resolution at 400 GHz, 0.11% resolution at 600 GHz, and 0.07% resolution at 800 GHz. Thus lower frequencies are more sensitive to corneal hydration changes than higher frequencies. These measurements can be combined with the noise parameters of a given THz imaging system to estimate the contrast that can be realized by any operational frequency band.

To estimate the sensitivity of the imaging system used in this research, the THz beam from the imaging system was focused onto a 1-mm piece of microscope glass ( $n \sim 2.11$  at 300 and 900 GHz)<sup>32</sup> and the reflected power was measured at 100 ms increments for 5 min. From the variance of this data, a noise-limited THz reflection sensitivity of  $\Delta R = 0.0275\%$  was computed. Therefore, the noise-equivalent water concentration change can be found by

$$\Delta C_{\text{H}_2\text{O}} = \frac{\Delta R}{\left(\frac{dR}{dC_{\text{H}_2\text{O}}}\right)}, \quad (5)$$

where  $C_{\text{H}_2\text{O}}$  is the water concentration,  $R$  is the THz reflectivity, and  $\Delta C_{\text{H}_2\text{O}}$  is the noise-equivalent water concentration sensitivity. This value was computed to be 0.190%, meaning that water concentrations of better than two parts in a thousand can be detected with this method. The estimated hydration sensitivity of

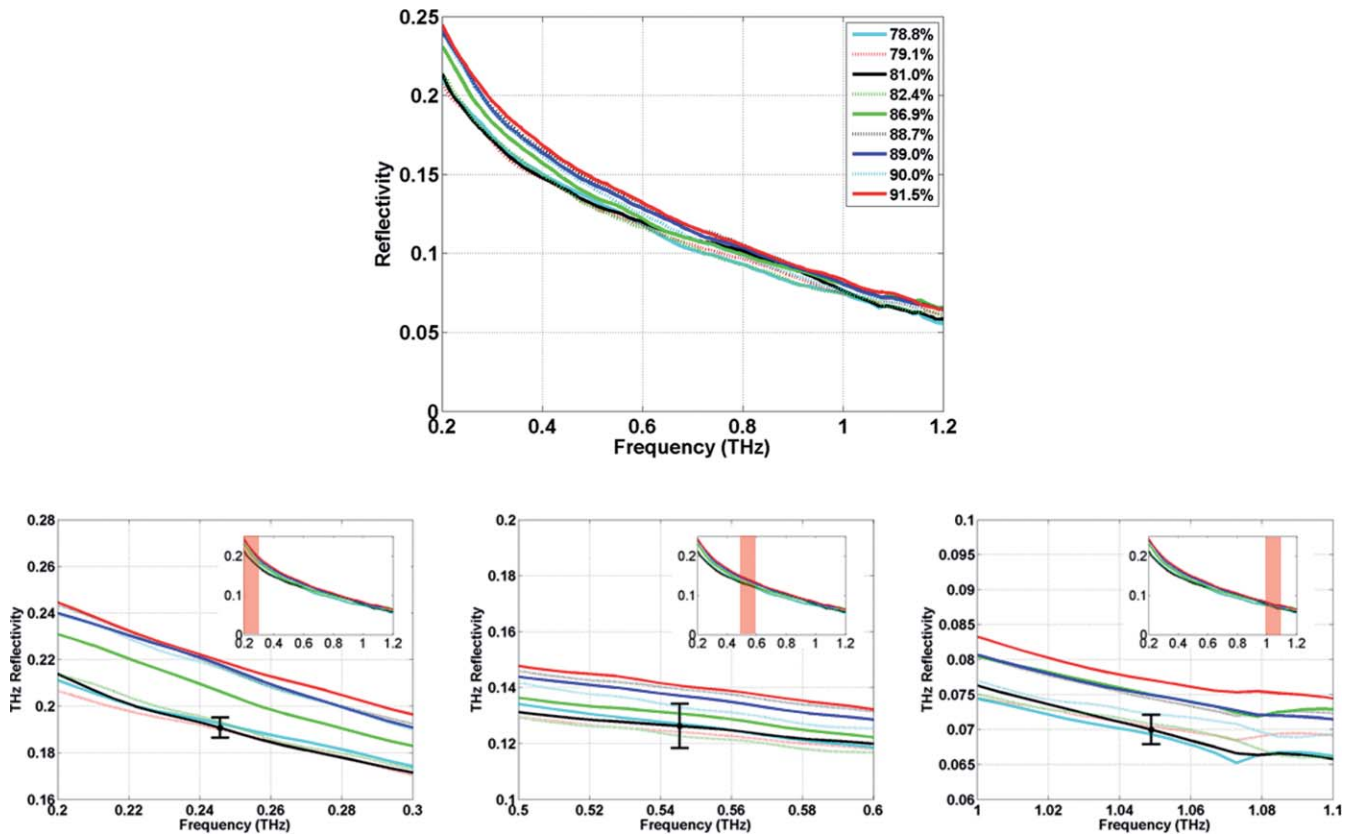


Fig. 4 THz spectra of ex-vivo porcine corneas prepared to uniform hydrations using PEG solutions.

optical and ultrasound pachymetry computed earlier was 0.5% and 0.4%, respectively [see Eq. (3)]. Thus the sensitivity computed here for THz sensing exceeds the theoretical performance of ultrasound and optical pachymetry by more than double.

### 3.3 Simulation of THz–Corneal Tissue Interaction and the Penetration Depth of THz Radiation in Corneal Tissues

The dielectric function of the composite of water and dry corneal tissue was modeled as described above and the simulated reflectivity is plotted in Fig. 7 alongside the measured THz reflectivity of a cornea at 79.1% water concentration. The measured and modeled reflectivity trends correspond very closely ( $R^2 = 0.977$ ), validating our use of the Bruggeman model.

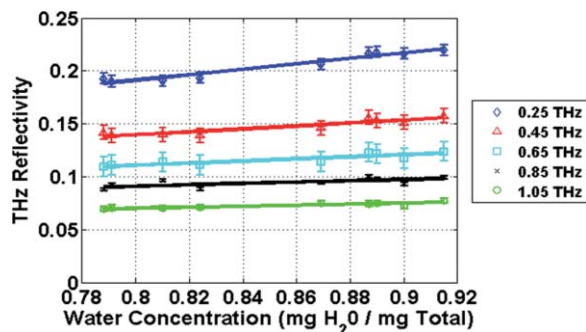


Fig. 5 THz reflectivity versus cornea concentration at 0.25, 0.45, 0.65, 0.85, and 1.05 THz shown alongside linear fits.

The effective combined permittivity computed for the composite cornea model (the effective media combination of water and dry corneal tissue) in this analysis can also be used to predict the depth in the cornea that can be interrogated by this technique. The simulated half-value layer of corneal tissue at 79.1% water concentration is shown in the bottom plot of Fig. 7. For example, at the center frequency of our imaging system,  $\delta_{HVL} \approx 81 \mu\text{m}$ . Thus the THz imaging system is predicted to interrogate roughly a few hundred micrometers of tissue and contains little influence

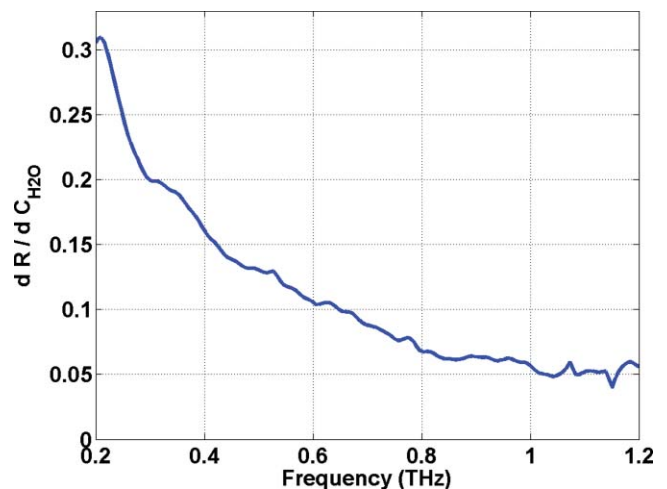


Fig. 6 Derivative of THz reflectivity with respect to water concentration, plotted against frequency.

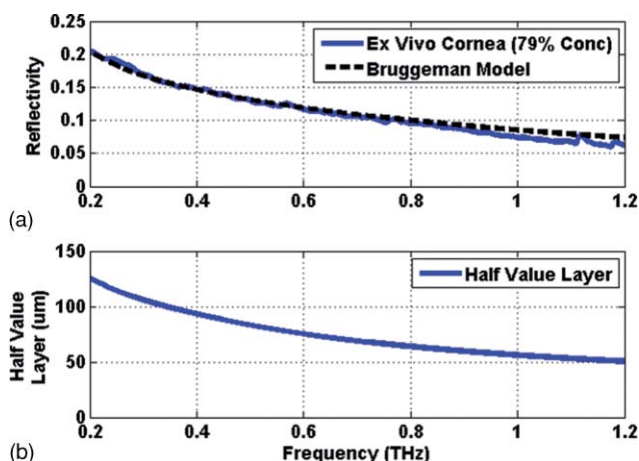


Fig. 7 (a) Measured and simulated reflectivity from a porcine cornea near physiological hydration. (b) Simulated half-value layer of THz radiation in corneal tissue.

from material behind the cornea (i.e., aqueous humor), where the signal for a round trip would be attenuated by  $>40$  dB.

This model also predicts that as the frequency falls below 50 GHz, the half-value layer rises above  $255 \mu\text{m}$  and the round trip loss drops to  $\sim 13$  dB. Therefore, radiation in the microwave frequency bands below  $\sim 50$  GHz are likely to significantly interact with the aqueous humor, and are not well suited to the task of corneal imaging.

This estimate of the penetration depth of the THz radiation tissue is critical to the discussion of THz hydration sensing because robust sampling of the cornea requires that the radiation interacts primarily in the corneal stroma without overshooting into the aqueous humor. Further, some disease processes exhibit depth-dependant hydration changes, and successful detection of these will require the selection of a probe frequency that can adequately penetrate to the appropriate depth for each. Direct measurement of the penetration depth is challenging because the attenuation in corneal tissue is very strong and it is difficult to detect radiation transmitted through whole cornea at THz frequencies. Future research will attempt to directly measure the penetration depth through thin slices of corneal tissue prepared to uniform thicknesses with a microkeratome and scanned immediately after harvesting to minimize the loss of tissue hydration through evaporation.

## 4 Discussion

There is currently no clinically-viable technology available to noninvasively assess the hydration changes characteristic of ocular diseases *in vivo*. Rough estimates of disease-related hydration changes can be obtained from available studies of disease-related CCT trends. First-order water concentration changes can be extrapolated from these CCT changes using the linear thickness-hydration relationship discussed earlier [Eq. (2)].

One potential application for THz hydration sensing is monitoring transplant patients for corneal graft rejection. Borderie et al followed the outcome of corneas undergoing transplant with 1-y CCTs of 500, 600, and  $700 \mu\text{m}$  and found that the 5-yr survival rate of these grafts were approximately 78%, 66%, and 48% respectively.<sup>14</sup> These thicknesses correspond to water

concentrations of 74.1%, 78.1%, and 81.0% with about a 2.5% concentration difference separating each, which is predicted to be well within the resolution abilities of our current THz imaging system. With sufficient hydration sensitivity, THz sensing may also be possible to image grafts exhibiting immunologic rejection and distinguish which of these grafts are likely to fail and which will recover. One study of 79 graft rejection patients found a significant difference between the mean thickness in grafts suffering from reversible and irreversible rejection events ( $681$  and  $774 \mu\text{m}$ ).<sup>33</sup> This represents a hydration difference of 2.2%, which is also an order of magnitude larger than the sensitivity obtained by our THz sensing system. Therefore this technology may be a valuable tool to study the risk factor, diagnosis, and prognosis of patients undergoing corneal transplants.

Hydration changes in Fuchs' dystrophy have also been considered. The mean CCT change observed in Fuchs' dystrophy is  $25 \mu\text{m}$ , which corresponds to a hydration change of about 1.00%.<sup>34</sup> The hydration changes in early-stage dystrophies occur at the endothelial side of the cornea, where the active pumping of water from the stroma is deteriorated. The corneal endothelium comprises the last cellular layer of the cornea, and an illuminating 0.525 THz beam must cross nearly 7 half-value layers to reach it and suffer a  $>40$  dB loss for the round trip back to the corneal surface. Thus, in order to fully realize a system capable of imaging early-stage dystrophies, a shift to deeper-penetrating lower frequencies and improvements to the system's SNR including increased source power and detector sensitivity may be necessary.

The utility of THz hydration monitoring to laser refractive surgeries applications is more difficult to analyze because the eye is held open during these procedures and significant depth-dependent variations are likely to arise. If the water concentration changes in the cornea during LASIK are assumed to be dominated by drying effects rather than by the effects of the excimer laser, then data from corneal drying studies can be leveraged to evaluate the potential of THz hydration monitoring. Confocal Raman spectroscopy data of rabbit eyes which are held open for extended periods of time are available, and these show that the majority of the drying takes place close to the surface.<sup>35</sup> Assuming an average cornea thickness of about  $410 \mu\text{m}$  in rabbits,<sup>36</sup> the volume of cornea within the predicted half-value layer of the surface exhibits an average water concentration change of 3.1% in 15 min and 5.4% in 45 min.<sup>35</sup> These long-time differences fall within the sensitivity capabilities of the THz sensing system, and it is expected that further improvements to the SNR of the system will only further improve the resolution.

## 5 Conclusion

THz imaging was successfully used to observe the evaporation of water from an *ex vivo* porcine cornea in a controlled set-up which isolated hydration-borne changes. These images confirm the existence of hydration-based contrast, and visualize the evaporation behavior in which water is lost from the outside edges—progressing—inward. The reflectivity changes inherent in corneal tissue of different water concentrations were measured from 150 to 1200 GHz, and a decreasing availability of contrast was observed at higher frequencies. This result can also be predicted using Bruggeman analysis which varies the water

concentration and computes the resulting effective media dielectric properties. This analysis predicts a decreasing half-value layer with increasing frequency, and suggests that THz imaging interrogates the first few hundred micrometers of corneal tissue. This property makes it very well suited for the evaluation of corneal hydration.

A key indicator of corneal health is found in its ability to properly regulate its water content, and deviations from normal hydration are significant indicators of many corneal disease processes. Monitoring water content may have clinical significance for diagnosis and disease monitoring in various corneal pathologies including dystrophies, degeneration, infection, inflammation, and graft rejection. The sensitivity of our THz imaging system was compared against several of these disease processes, and predicted to be more than adequate for diagnostic imaging and hydration sensing in corneal graft rejection and laser refractive surgery tasks. This research effort will also continue to benefit from ongoing advancements in THz power output and detector sensitivity which will increase the sensitivity of THz monitoring to small hydration changes as well as its useful imaging depth, and further add to the potential of this technology as a diagnostic tool in clinical ophthalmology.

### Acknowledgments

This work was supported by the Telemedicine and Advanced Funding provided by the Telemedicine and Advanced Technology Research Center, Department of Defense under award number W81XWH-09-2-0017, a student research grant from the American Society of Lasers in Medicine and Surgery, and a graduate student fellowship through the UCLA Electrical Engineering Department. This material is also based in part upon work supported by the National Science Foundation under Grant Nos ECCS-801897. Any opinions, findings, and conclusions or recommendations expressed in this material are those of the authors and do not necessarily reflect the views of the National Science Foundation.

### References

1. E. Pickwell and V. P. Wallace, "Biomedical applications of terahertz technology," *J. Phys. D: Appl. Phys.* **39**, R301–R310 (2006).
2. R. M. Woodward, V. P. Wallace, R. J. Pye, B. E. Cole, D. D. Arnone, E. H. Linfield, and M. Pepper, "Terahertz pulse imaging of ex vivo basal cell carcinoma," *J. Invest. Dermatol.* **120**(1), 72–78 (2003).
3. E. Berry, J. W. Handley, A. J. Fitzgerald, W. J. Merchant, R. D. Boyle, N. N. Zinov'ev, R. E. Miles, J. M. Chamberlain, and M. A. Smith, "Multispectral classification techniques for terahertz pulsed imaging: an example in histopathology," *Med. Eng. Phys.* **26**(5), 423–430 (2004).
4. R. M. Woodward, B. E. Cole, V. P. Wallace, R. J. Pye, D. D. Arnone, E. H. Linfield, and M. Pepper, "Terahertz pulse imaging in reflection geometry of human skin cancer and skin tissue," *Phys. Med. Biol.* **47**(21), 3853–3863 (2002).
5. V. P. Wallace, A. J. Fitzgerald, S. Shankar, N. Flanagan, R. Pye, J. Cluff, and D. D. Arnone, "Terahertz pulsed imaging of basal cell carcinoma ex vivo and in vivo," *Br. J. Dermatol.* **151**(2), 424–432 (2004).
6. D. Mittleman, "Terahertz imaging," in *Sensing with Terahertz Radiation*, Springer Ser. Opt. Sci. Vol. 85, D. Mittleman, Ed., pp. 131–145, Springer, Berlin (2003).
7. M. J. Dougherty and M. L. Zaman, "Human corneal thickness and its impact on intraocular pressure measures: a review and meta-analysis approach," *Surv. Ophthalmol.* **44**(5), 367–408 (2000).
8. P. M. Kiely, G. Smith, and L. G. Carney, "The mean shape of the human cornea," *Optica Acta: Int J Optics* **29**(8), 1027–1040 (1982).
9. R. M. Robb and T. Kuwabara, "Corneal wound healing: I. the movement of polymorphonuclear leukocytes into Corneal Wounds," *Arch. Ophthalmol.* **68**(5), 636–642 (1962).
10. B. O. Hedbys and S. Mishima, "Flow of water in the corneal stroma," *Exp. Eye Res.* **1**, 262–275 (1962).
11. J. Ytteborg and C. H. Dohlman, "Corneal edema and intraocular pressure: II. clinical results," *Arch. Ophthalmol.* **74**(4), 477–484 (1965).
12. N. Rosa, M. Lanza, M. Borrelli, M. L. Filosa, M. D. Bernardo, V. M. Ventriglia, M. R. Cecio, and L. Politano, "Corneal thickness and endothelial cell characteristics in patients with myotonic dystrophy," *Ophthalmol* **117**(2), 223–225 (2010).
13. B. Lackner, G. Schmidinger, S. Pieh, M. A. Funovics, and C. Skorpik, "Repeatability and reproducibility of central corneal thickness measurement with Pentacam, Orbscan, and ultrasound," *Optometry Vision Sci.* **82**(10), 892–899 (2005).
14. V. M. Borderie, O. Touzeau, T. Bourcier, C. E. Allouch, E. Zito, and L. Laroche, "Outcome of graft central thickness after penetrating keratoplasty," *Ophthalmol.* **112**(4), 626–633 (2005).
15. P. J. Dougherty, K. L. Wellish, and R. K. Maloney, "Excimer laser ablation rate and corneal hydration," *Am. J. Ophthalmol.* **118**(2), 169–176 (1994).
16. E. R. Brown, A. W. M. Lee, B. S. Navi, and J. E. Bjarnason, "Characterization of a planar self-complementary square-spiral antenna in the THz region," *Microwave Opt. Technol. Lett.* **48**(3), 524–529 (2006).
17. Z. D. Taylor, R. S. Singh, M. O. Culjat, J. Y. Suen, W. S. Grundfest, H. Lee, and E. R. Brown, "Reflective terahertz imaging of porcine skin burns," *Opt. Lett.* **33**(11), 1258–1260 (2008).
18. R. S. Singh, Z. D. Taylor, P. Tewari, D. Bennett, M. O. Culjat, H. Lee, E. R. Brown, and W. S. Grundfest, "THz Imaging of Skin Hydration: Motivation for the Frequency Band," in *SPIE BIOS: Adv. Biomed. Clin. Diagn. Syst. VIII, San Francisco, CA* (2010).
19. D. B. Bennett, Z. D. Taylor, S. Sung, N. Bajwa, B. Makkabi, R. S. Singh, P. Tewari, M. O. Culjat, W. S. Grundfest, and E. R. Brown, "Terahertz time-lapse video of hydration in physiological tissues," in *SPIE BIOS, San Francisco, CA* (2011).
20. K. M. Meek, N. J. Fullwood, P. H. Cooke, G. F. Elliott, D. M. Maurice, A. J. Quantock, R. S. Wall, and C. R. Worthington, "Synchrotron x-ray diffraction studies of the cornea, with implications for stromal hydration," *Biophys. J.* **60**(2), 467–474 (1991).
21. S. Krishnamurthy, M. T. Reiten, S. A. Harmon, and R. A. Cheville, "Characterization of thin polymer films using terahertz time-domain interferometry," *Appl. Phys. Lett.* **79**(6), 875–877 (2001).
22. D. B. Bennett, W. Li, Z. D. Taylor, W. S. Grundfest, and E. R. Brown, "Stratified media model for Terahertz reflectometry of the Skin," submitted, *IEEE Sens. J.* **11**(5), 1253–1262 (2010).
23. J. T. Kindt and C. A. Schmittenmaer, "Far-infrared dielectric properties of polar liquids probed by femtosecond Terahertz pulse spectroscopy," *J. Phys. Chem.* **100**(24), 10373–10379 (1996).
24. D. M. Maurice, "The structure and transparency of the cornea," *J. Physiol.* **136**(2), 263–286 (1957).
25. S. Mishima and B. O. Hedbys, "Physiology of the Cornea," *Int. Ophthalmol. Clin.* **8**(3), 527–560 (1968).
26. F. H. Attix, *Introduction To Radiological Physics And Radiation Dosimetry*, Wiley, New York (1986).
27. J. W. Lamb, "Miscellaneous data on materials for millimetre and submillimetre optics," *Int. J. Infrared Millimeter Waves* **17**(12), 1997–2034 (1996).
28. B. A. Holden, J. J. McNally, and P. Egan, "Limited lateral spread of stromal edema in the human cornea fitted with a ('donut') contact lens with a large central aperture," *Curr. Eye Res.* **7**(6), 601–605 (1988).
29. R. S. Singh, P. Tewari, J. L. Bourges, J. P. Hubschman, D. B. Bennett, Z. D. Taylor, H. Lee, E. R. Brown, W. S. Grundfest, and M. O. Culjat, "Terahertz sensing of corneal hydration," in *32nd Annual International Conference IEEE Eng. Med. Biol. Society, Buenos Aires* (2010).
30. G. A. Niklasson, C. G. Granqvist, and O. Hunderi, "Effective medium models for the optical-properties of Inhomogeneous Materials," *Appl. Opt.* **20**(1), 26–30 (1981).



31. K. K. Karkkainen, A. H. Sihvola, and K. I. Nikoskinen, "Effective permittivity of mixtures: Numerical validation by the FDTD method," *IEEE Trans on Geosci Remote Sens.* **38**(3), 1303–1308 (2000).
32. M. Halpern, H. P. Gush, E. Wishnow, and V. De Cosmo, "Far infrared transmission of dielectrics at cryogenic and room temperatures: glass, Fluorogold, Eccosorb, Stycast, and various plastics," *Appl. Opt.* **25**(4), 565–570 (1986).
33. H. G. M. D. Naacke, V. M. M. D. P. D. Borderie, T. M. D. Bourcier, O. M. D. Touzeau, M. M. D. Moldovan, and L. M. D. Laroche, "Outcome of Corneal Transplantation Rejection," *Cornea* **20**(4), 350–353 (2001).
34. R. Mandell, K. Polse, R. Brand, D. Vastine, D. Demartini, and R. Flom, "Corneal hydration control in Fuchs' dystrophy," *Invest. Ophthalmol. Vis. Sci.* **30**(5), 845–852 (1989).
35. N. Bauer, J. Wicksted, F. Jongsma, W. March, F. Hendrikse, and M. Motamedi, "Noninvasive assessment of the hydration gradient across the cornea using confocal Raman spectroscopy," *Invest. Ophthalmol. Vis. Sci.* **39**(5), 831–835 (1998).
36. T. Chan, S. Payor and B. Holden, "Corneal thickness profiles in rabbits using an ultrasonic pachometer," *Invest. Ophthalmol. Vis. Sci.* **24**(10), 1408–1410 (1983).